The Effects of Embroidery Parameters upon Processing and Mechanical Properties of Cornely Embroidered Quasi-Unidirectional Reinforcement.

D. J. Morris, C. D. Rudd, S. P. Gardner and N. A Warrior,

Department of Mechanical Engineering,
The University of Nottingham,
University Park,
Nottingham.
NG7 2RD

Abstract

A Cornely embroidery machine was used to produce quasi-unidirectional glass reinforcement consisting of glass fibre rovings wrapped helically by a polyester thread, then stitched to a plain woven glass substrate by a polyester chain stitch. The glass filament diameter was varied, along with the coiling frequency and tension in the wrapping thread in order to assess the effects of embroidery variables on processing. In-plane permeability tests were performed on dry reinforcement. Moulded plaques were examined under a microscope to assess void content and wet-out, and tensile and flexural tests were performed. Results were compared with plaques from a commercially available quasi-unidirectional stitch-bonded non-crimp fabric (NCF). Improvements in 0° tensile modulus and strength were observed for the embroidered reinforcement over the NCF. An increase in filament diameter showed a decrease in void content, and a corresponding increase in mechanical properties. Higher wrapping stitch frequencies gave improved properties, while the wrapping thread tension had no significant effect upon processing or mechanical properties.

1. Introduction

Conventional reinforcement techniques used in fibre reinforced plastics tend not to take full advantage of the anisotropic nature of the mechanical properties of composite materials. For components with well defined load cases, such as struts, pressure vessels and torsion shafts, fibre distributions which align the reinforcing fibres with the principal stress directions can be achieved straightforwardly using methods such as filament winding, or using aligned reinforcement fabrics. For components with more complex load cases, such as those that arise around loading points or inspection holes, local reinforcement can be used with some success, such as the inclusion of bonded or cold-expanded metallic inserts around holes[1,2]. Previous attempts at controlling fibre architecture around circular holes, such as the deformation of woven reinforcements by insertion of a pointed steel punch have also demonstrated improvements in mechanical properties[3], though placement of local reinforcement by hand is both labour-intensive and subject to operator influence. One method of addressing this is to use textile processes to produce reinforcements with fibre directions which are tailored to the application, rather than fabrics with the same global fibre orientations. Some scope exists in weft knitting[4], though the static properties of the resultant mouldings tend to be lower than those of random reinforcements, 3D weaving[5], though this is generally limited to three orthogonal axes, and embroidery.

Embroidery in its highly mechanised form has existed for over 130 years, since Isaak Groebli of Oberuzwyl, Switzerland combined the labour intensive process of handloom embroidery with the high productivity of the recently popular sewing machine[6]. The handloom duplicated the action of sewing by hand, passing one thread back and forth through the carrier material, whilst the sewing machine utilised two threads, a front yarn threaded through the needle, and yarn on a bobbin to lock the front yarn at the rear face of the carrier. Groebli saw that by using two interlocking threads, the enormous potential of automating the embroidery process for the mass production of intricate designs could be realised.

The two main approaches to embroidery are (i) stitching through a substrate material to produce a motif with the stitching thread itself, or (ii) tacking a heavier cord to a substrate using a stitching thread so that the cord forms the motif. Both of these processes offer considerable potential for composites manufacture since each could be realised by the use of appropriate reinforcement fibres for either stitching through, or tacking to a carrier material. Figures 1 and 2 demonstrate applications of both of these processes. Each approach can be applied locally to reinforce a part of a preform, or globally to produce an entire preform with the potential to place fibres accurately and repeatably where desired, with little or no waste. Textile embroidery processes are sufficiently advanced that rapid component development times are available due to existing links with CAD software, and a high degree of automation and mechanisation offers good reproducibility for a low labour input.

The embroidery process can be applied to the manufacture of composites in a variety of ways. Dry reinforcement can be prepared for liquid moulding processes, alternatively pre-pregged reinforcement, or hybrid yarns for thermoplastic matrix composite preforms. Substrates can be either permanent and structural, such as a woven or stitch-bonded reinforcement fabric as seen in Figure 1, permanent and non-structural such as a nylon mesh as seen in Figure 2, or soluble using an alginate or an acetate film. Some of these applications have been demonstrated, by Drummond[7], and by Gleische and Rothe[8], and patents describing processes where reinforcement filaments are tacked down by a stitching thread have been applied for in both Germany[9] and Japan[10]. Despite the apparent potential, no results have been published demonstrating properties of composites manufactured from embroidered preforms.

Certain issues arise from the use of different embroidery processes, such as Cornely or Schiffli, for the production of composite reinforcement. The Cornely machine consists of a horizontal frame in which the carrier material is located, and one or several fixed stitching heads. The frame size depends on the number of stitching heads, at around ¼m² per head. The movement of the frame is controlled electronically, along with the reciprocating motion of the needle. The Schiffli machine also consists of a frame locating the carrier material, though the frame is located vertically. Multiple needles are mounted along the length of the frame, so a design may be repeated on a single carrier material. The frame can be up to 30m in length and 2 m in height, with needles spaced as little as 20-30mm apart, facilitating high volume production. The Cornely machine is used for both stitching and tacking down of a heavy cord, whereas the Schiffli is used purely for stitching. Suitable yarns and substrates which can tolerate the aggressive nature of the stitching process must be identified, and the permeability and formability characteristics of the resulting reinforcement assessed. The quality of the fibre distribution, both the dimensional tolerance of the lay-down and in the cross-section of the laminate, also require investigation, along with the mechanical properties of the laminate. In order to exploit the full potential of local control over fibre architecture, suitable design and analysis methods must be identified, and the economics of the process investigated.

The work described in this paper arises from a collaborative project looking at the feasibility of automotive and aerospace applications of the embroidery process. Initially, the most basic unidirectional structure was studied to provide understanding and to generate property data to apply to more complex design cases.

For this investigation, embroidered samples were produced on a single-head Cornely embroidery machine. All embroidered reinforcement samples consisted of 2400 tex glass fibre roving embroidered 2mm between centres onto a 200g/m^2 plain woven glass substrate, using a polyester sewing thread. The construction is shown schematically in Figure 3, and an electron micrograph shown in Figure 4. The embroidery variables chosen for study were the glass fibre diameter, the frequency of the helical wrap, and the tension in the helical wrapping thread. These variables are summarised below in Table 1.

Sample Type Identifier	Glass Filament Diameter (μm)	Helical Wrapping Stitch Frequency (stitches/wrap)	Stitch Tension
A	13	3	High
B	17	3	Low
C	13	6	Low
D	17	6	High

Table 1: Embroidered reinforcement sample list.

For comparison purposes, a commercially available non-crimp glass fibre fabric (NCF), Tech Textiles E-LPb 567 (style 1038), was examined. This is a stitch bonded fabric; 90% of the fibres lie in the machine (warp) direction, stitched to the 10% that lie in the transverse (weft) direction for stability. The glass filament diameter of the NCF was 11μm. The construction of this fabric is shown schematically in Figure 5, and an electron micrograph shown in Figure 6.

In order to assess the processing properties of these reinforcements, in-plane permeability tests were performed, along with void analysis of cross-sections of moulded plaques by optical microscopy. Mechanical testing was also performed to assess ultimate tensile strength (UTS), Young's modulus, flexural modulus, and inter-laminar shear strength (ILSS).

2. Experimental Details

2.1 In-Plane Permeability Measurement

The experimental apparatus used for in-plane permeability measurement consisted of a circular cavity of diameter 400mm, depth 4mm, with a central inlet of diameter 10mm. Pressure transducers were located along two orthogonal axes, at 55mm, 110mm and 165mm from the centre of the cavity, and a thermocouple located beside the inlet gate. Layers of reinforcement material were stacked, a central hole of diameter 10mm was punched, and the stacked reinforcement was placed in the cavity. An aluminium lid and arrangement of stiffening bars were bolted down on top, to simulate a closed mould. A cylinder of bore 160mm was situated in an Instron 1195 universal testing machine, such that the vertical movement of the cross-head caused a piston to push SAE 30 oil out of the cylinder at closely controlled flow rate. The oil

was injected through the 10mm diameter inlet hole in the centre of the cavity. Pressures and temperatures were logged during injection by a 386 PC running Intelligent Instrumentation Visual Designer. Upon completion of injection, pressures logged from each transducer were plotted against ½ln(time), and fitted with straight lines of characteristic gradient, from which principal permeability values were calculated, according to a method proposed by Chick *et al*[11]. Two permeability tests were performed on each type of embroidered reinforcement, and results are shown in Table 2. Principal permeability values for the NCF are shown for comparison, and were obtained by extrapolation of a curve of the form $y=Ax^B$ fitted through data obtained from experimentation as described in Section 2.1 over a range of volume fractions from 22% to 38%.

2.2 Manufacture of Plaques

All plaques were manufactured in an aluminium mould of dimensions 90mm x 250mm x 3.5mm. Reinforcement samples were cut carefully to an exact fit, to minimise the possibility of resin flowing preferentially in any gaps between the preform and the mould wall, which could lead to dry patches in the moulding. The NCF preforms contained of 7 layers of reinforcement, with all layers in the same orientation, as shown in Figure 7. The embroidered preforms contained 3 layers of embroidered reinforcement, such that a substrate layer was situated on both outer faces, shown in Figure 8. Cray Valley CVP 6345.001 polyester resin with 2% Perkadox 16 catalyst was injected under a vacuum of 850-900 mbar, and distributed along the width of the preform by a line reservoir. Upon filling, the inlet and vent were sealed, and the mould tool placed in an oven to cure at 70°C for 2 hours. The cured samples were post cured at 115°C for 4 hours. All plaques were moulded at a nominal glass volume fraction of 45%.

2.3 Void Counting

Cross-sectional microscopy specimens were prepared from each plaque, and polished using progressively finer abrasives, to a grade of 1 micron using alumina paste. Digital images at a magnification of x20 were obtained, and examined to assess the fibre distribution, and the void content of each plaque. Void content was assessed by superimposing a rectangular grid of 15 x 20 squares onto the images, and calculating the percentage of grid points coinciding with apparent voids, identified as dark spots on the images[12].

2.4 Mechanical Testing

Tensile[13] and flexural[14] testing was performed according to BS2782, in an Instron universal testing machine, model 1195. The results of these tests yielded values of ultimate tensile strength (UTS), Young's modulus, interlaminar shear strength (ILSS), and a flexural modulus for comparison.

3. Results and Discussion

3.1 In-Plane Permeability

Permeability results are shown in Table 2. Embroidered samples B and D have principal permeabilities higher than those of samples A and C, suggesting that the larger roving filament

diameter (17μm) has a beneficial effect on permeability. It is thought that this is due to the geometry of the packing of the filaments within the compacted reinforcement; larger filaments will tend to pack with larger channels between them, leading to larger cross-sectional hydraulic radii available for flow. Due to the improvement in apparent permeability of sample type B over sample type D, particularly in the weft (y) direction, the combination of a wrapping stitch every 3 chain stitches coupled with a low tension in the wrapping thread appears to be beneficial. Results of sample types A and C are similar, suggesting that the effects on permeability of the stitch tension and stitch frequency are equal. The relatively higher permeability of sample type B suggests that the contributions of stitch tension and frequency are less dominant than the effect of roving filament diameter.

Sample Type	Porosity	Warp permeability Kx (m^2)	Weft permeability Ky (m^2)
A	0.6	2.71E-11	7.17E-12
A	0.6	2.95E-11	7.81E-12
B	0.6	5.89E-11	1.65E-11
B	0.6	5.23E-11	1.47E-11
C	0.6	3.19E-11	7.97E-12
C	0.6	3.05E-11	7.62E-12
D	0.6	5.53E-11	9.09E-12
D	0.6	4.26E-11	7.51E-12
NCF	0.6	1.37E-10	7.16E-12

Table 2: In-plane permeability results for embroidered reinforcement and NCF.

Results for the NCF demonstrate permeability along the warp (x) direction to be around 4 to 8 times greater than that of the embroidered reinforcement. In the weft (y) direction, the NCF permeability is similar to that of the embroidered reinforcements, showing the higher degree of anisotropy inherent in the commercially available fabric. This is thought to be due to the channels in the warp direction down which fluid may flow more readily than within the fibre tows. As a result the flow within the fibre tows will tend to lag behind flow in the channels between tows, which could lead to problems of air entrapment (intra-tow voidage) as described by Patel and Lee[15]. In studies of fabrics with flow-enhancing properties, such as warp-bound and twisted tows (providing channels for preferential flow), Summerscales *et al*[16] have demonstrated a reduction in mechanical properties of laminates with increasing proportion of flow-enhancing tows, which has been attributed to a similar flow mechanism.

As described in Section 1, the embroidered reinforcement was constructed from unidirectional roving and an orthotropic plain woven substrate. Permeability tests upon the substrate yielded principal permeability values of the same order as the weft direction permeability results for the embroidered reinforcement (around 10^{-12}). It is likely that the flow mechanism in the warp direction of the embroidered reinforcement is dominated by the flow within and around the roving, and the permeability in the weft direction is dominated by flow within the substrate. Despite having a smaller proportion of fibres in the weft direction, the embroidered reinforcement appears less anisotropic during flow than the NCF.

3.2 Laminate Quality

Results from void counting are shown in Table 3. It can be seen that again, embroidered reinforcement type B performs best, and type C performs least well. The void count for the NCF suggest that it performs similarly to embroidered sample type B. Each micrograph demonstrated good wet out of the fibre tows and voids tended to be situated in the more densely packed regions, between glass filaments (intra-tow voidage).

Sample Type	Mean Void Content (%)	Standard deviation
A	0.645	0.224
B	0.347	0.224
C	0.843	0.293
D	0.397	0.243
NCF	0.397	0.243

Table 3: Void content results for embroidered reinforcement and NCF plaques.

3.3 Laminate Mechanical Properties

(a) Tensile Properties

Type	Mean UTS (MPa)	Standard Deviation	Mean E (GPa)	Standard Deviation
A	695.6	13.9	34.03	0.10
B	762.5	11.9	36.99	0.93
C	606.5	1.6	31.56	0.47
D	702.9	13.4	34.34	0.43
NCF	462.4	10.5	30.24	0.48

Table 4: Tensile test results for embroidered reinforcement and NCF plaques.

Results of the tensile tests are shown in Table 4. Embroidered samples B and D made from 17mm filament diameter roving demonstrate higher UTS than embroidered samples A and C made from smaller filament diameter roving (13mm). This improvement is also evident in results for Young's modulus, samples B and D again being higher than samples A and C. It was expected that the smaller filament diameter glass would perform better than the larger filament diameter, as the smaller filaments would have a higher surface area available for adhesion to the matrix. A larger area of interface should lead to a reduction in interfacial stress, therefore a stronger composite. Also, the larger filaments have a larger critical bend radius (minimum radius round which they may be turned before breaking), which would lead to them being more easily damaged during processing. It is likely that the differences in void content between embroidered sample types influenced their relative performance, as suggested by Judd and Wright[12], so the improved processibility of reinforcement type B was more significant than the theoretical improvement offered by smaller filaments. The inclusion of a wrapping thread every 3 chain stitches also appears to have a beneficial effect on these properties, seen in the relative difference in both UTS and Young's modulus between samples

B and C, and the relative similarity of samples A and D. The wrapping stitch tension in the embroidered reinforcement appears to have little effect on either UTS or Young's modulus. All samples made from embroidered reinforcement appear to have a higher UTS than those made from the NCF. The range of improvement is from sample type C, which demonstrates a 30% increase in UTS, to sample type B, which demonstrates a 65% increase. Embroidered reinforcement samples also demonstrate an increase in Young's modulus over the NCF which showed 30GPa, from a 5% increase (sample type C) to a 20% increase (sample type B). Some improvements in longitudinal tensile properties were expected as the embroidered reinforcement had a larger percentage of the total reinforcement in the warp direction (93%) than the NCF (90%), though the magnitude of the improvements suggests that effects must be attributed to the embroidery parameters also. Basford *et al*[17] have demonstrated experimentally a degradation of mechanical properties with an increased proportion of clustered tows. This corresponds to the microstructure of the NCF, where resin rich channels form between fibre tows, compared with the embroidered reinforcement, which compacts to give a more even distribution of fibres. The most significant conclusion from these tests is therefore the relative improvement in tensile mechanical properties of the embroidered reinforcement over the NCF.

(b) Flexural Properties

Type	Mean ILSS (MPa)	Standard Deviation	Mean Flexural Modulus (GPa)	Standard Deviation
A	16.05	0.68	27.65	0.67
B	15.42	1.09	32.58	1.28
C	14.13	0.49	26.83	0.53
D	16.55	0.38	30.30	0.66
NCF	16.93	2.08	23.84	1.87

Table 5: Flexural test results for embroidered reinforcement and NCF plaques.

Results of flexural testing are shown Table 5. The ILSS test results show that reinforcements A, B and D perform similarly to the NCF, though sample type C appears to have a lower ILSS. Results from flexural modulus testing are in line with results from void counting and tensile testing, sample types B and D demonstrating improved properties over sample types A and C. Results from the NCF demonstrate a flexural modulus similar to embroidered sample types A and C. Again it is likely that the dominant effect on the distribution of the mechanical property data is void content, as discussed above in Section (a). Also, the different stacking sequences as shown in Figures 7 and 8 cause a difference in fibre distribution in the cross section, so a direct comparison of flexural properties is not possible.

4. Conclusions

For the embroidered reinforcement, results from void counting complement those from mechanical and permeability tests, with embroidered sample type B demonstrating the lowest void count, and sample type C the highest. Voids within composite components have been shown to decrease mechanical properties[12], particularly at void contents between 0% and 1%, and it is probable that this is the dominant effect observed within the data. It is likely, therefore, that the embroidery parameters associated with sample type B lead to a relatively

more easily and evenly impregnated composite. This may be due to the flow mechanisms involved since larger filament diameter roving and a more frequent wrapping stitch leading to higher permeability. However more investigation at a variety of volume fractions is necessary for confirmation.

The relative improvement in mechanical properties of each type of embroidered reinforcement over the NCF appears to be due to the reinforcement architecture, which was more clustered in the NCF. Void counting suggested that the NCF performed as well as embroidered reinforcement type B.

Overall, the unidirectional reinforcement embroidered onto a woven substrate performs in a similar manner to a non-crimp fabric, with improvements in fibre distribution leading to marginal improvements in mechanical properties. The embroidered reinforcement has the potential advantage of close control over reinforcement microstructure, making it attractive as a means of preform production for composites.

Acknowledgements

Thanks to AK Kingham, RC Smith, and A Seadon for their invaluable assistance during this work. Acknowledgements are also due to the partners of the MASCET project, funded under the LINK Structural Composites Programme:
Ford Motor Company, Hewetson-Leveaux Ltd, Cray Valley Totale Ltd, G E Macpherson Ltd, PPG Industries UK Ltd, Lucas Applied Technology Ltd, Crescent Consultants Ltd, Tenax Fibres Ltd, Vidhani Brothers Ltd, Ellis Developments Ltd., EPSRC and Dept. of Trade and Industry.

References

1. Herrera-Franco, PJ, Cloud, GL, "Strain relief inserts for composite fasteners - an experimental study" Journal of Composite Materials, Vol26 No5, 1992, pp751-768

2. Rufin, AC, "Fastener hole reinforcement in composites using cold-expanded inserts" Journal of Composites Technology and Research, Vol17 No2, 1995, pp145-151

3. Chang, L-W, Yau, S-S, Chou, T-W, "Notched strength of woven fabric composites with moulded-in holes" Composites, Vol18 No3, Jul. 1987, pp233-241

4. Rudd, CD, "Preform processing for high volume resin transfer moulding" Ph.D. Thesis, University of Nottingham, 1989

5. Brosius, P, Clarke, S, "Textile preforming techniques for low cost structural composites" Adv. Comp. Matls., Apps. Conf. Proc. Detroit, MI, USA, Sep. 30 - Oct. 3 1991, pp1-10

6. Schneider, C, "Embroidery: Schiffli and multi-head", C Schneider, 1978

7. Drummond, T, "Automated near-net preform manufacturing for high speed resin transfer moulding" pp373-376

8. Gleische, K, Rothe, H, "Textile constructions for composite parts with stress field aligned fiber placement" Presented at "Textiles for Composites Workshop and Research Discussion", UMIST, UK 19-20 Oct. 1994

9. Inst. Polymerforschung Dresden EV, EP 567845-A1, European Patents Abstracts, Week 9344, pp87

10. Japanese Patent Specification No. 11339/1985 (60-11339) - Method of making fibre-reinforced composite material

11. Chick, JP, Rudd, CD, "Material characterization for flow modeling in structural reaction injection molding" Polymer Composites, Vol17 No1, Feb. 1996, pp124-135

12. Judd, NCW, Wright, WW, "Voids and their effects on the mechanical properties of composites - an appraisal", SAMPE Journal, Jan/Feb. 1978, pp10-14

13. British Standards Institute, BS2782 (EN61) Part 10: Method 1003:1977, "Determination of tensile properties"

14. British Standards Institute, BS2782 (EN63) Part 10: Method 1005:1977, "Determination of flexural properties. Three point method"

15. Patel, N, Lee, LJ, "Effects of fiber mat architecture on void formation and removal in liquid composite moulding" Polymer Composites, Vol16, No5, Oct. 1991, pp386-399

16. Summerscales, J, Griffin, JR, Grove, SM, Guild, FJ, "Quantitative microstructural examination of RTM fabrics designed for enhanced flow" Composite Structures, Vol32 No1-4, 1995, pp519-529

17. Basford, DM, Griffin, PR, Grove, SM, Summerscales, J, "Relationship between mechanical performance and microstructure in composites fabricated with flow-enhancing fabrics" Composites, Vol26, No9, 1995, pp675-679

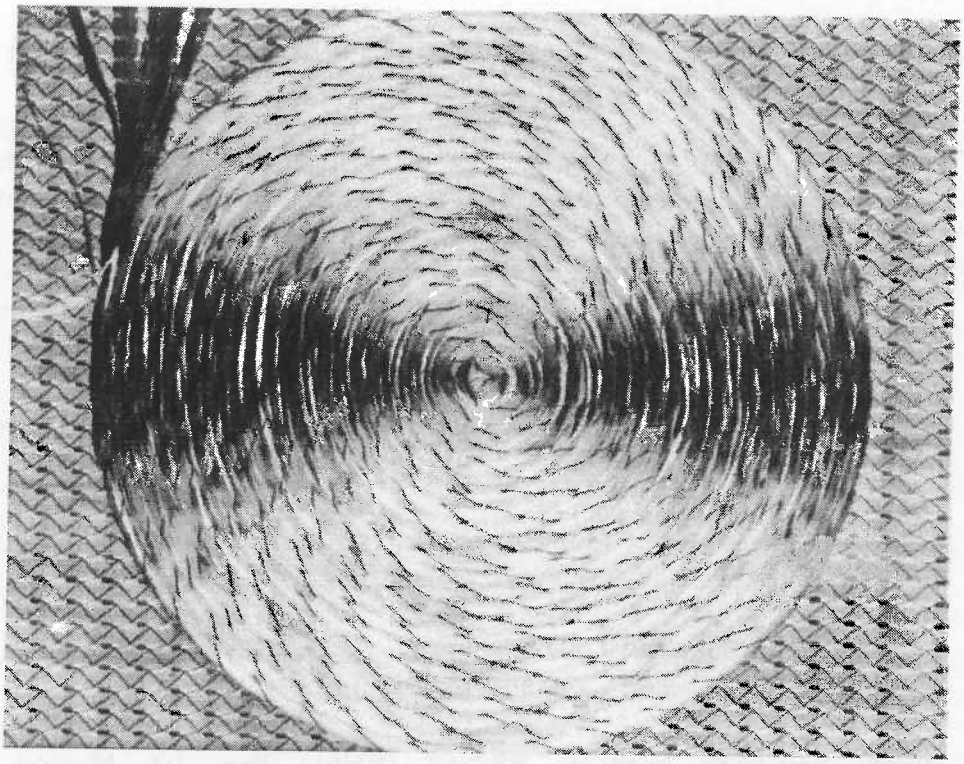

Figure 1: **2400tex glass roving tacked onto stitch-bonded glass fabric by polyester stitching thread.**

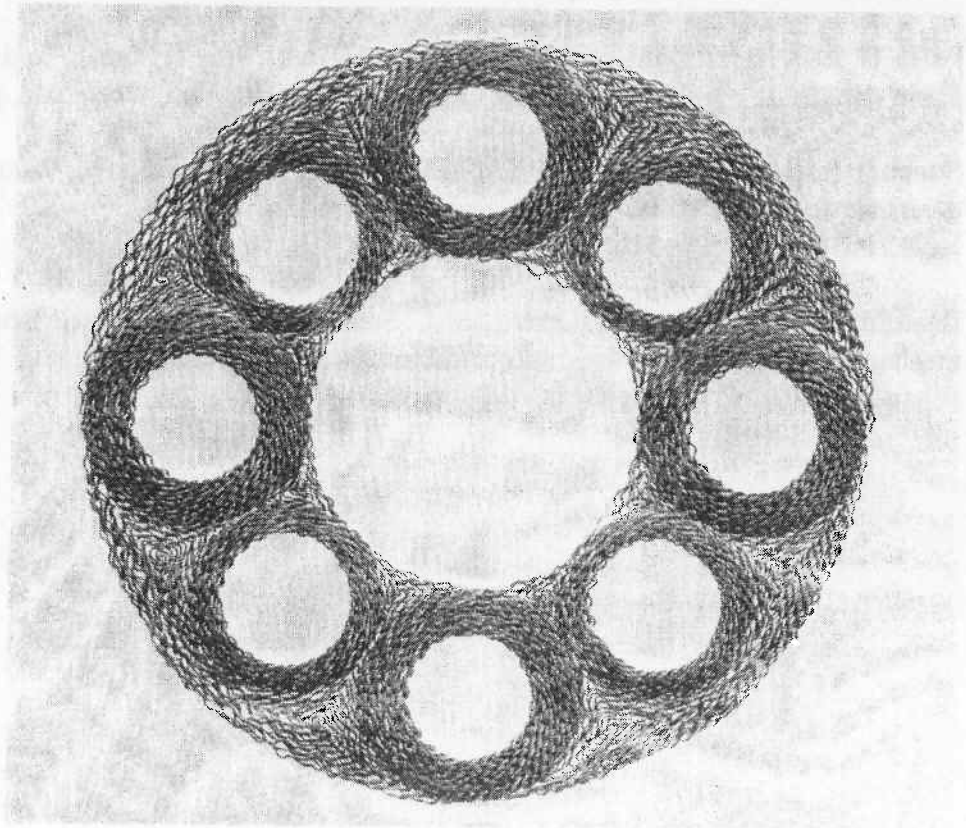

Figure 2: **Aramid fibres stitched by embroidery onto a nylon mesh substrate.**

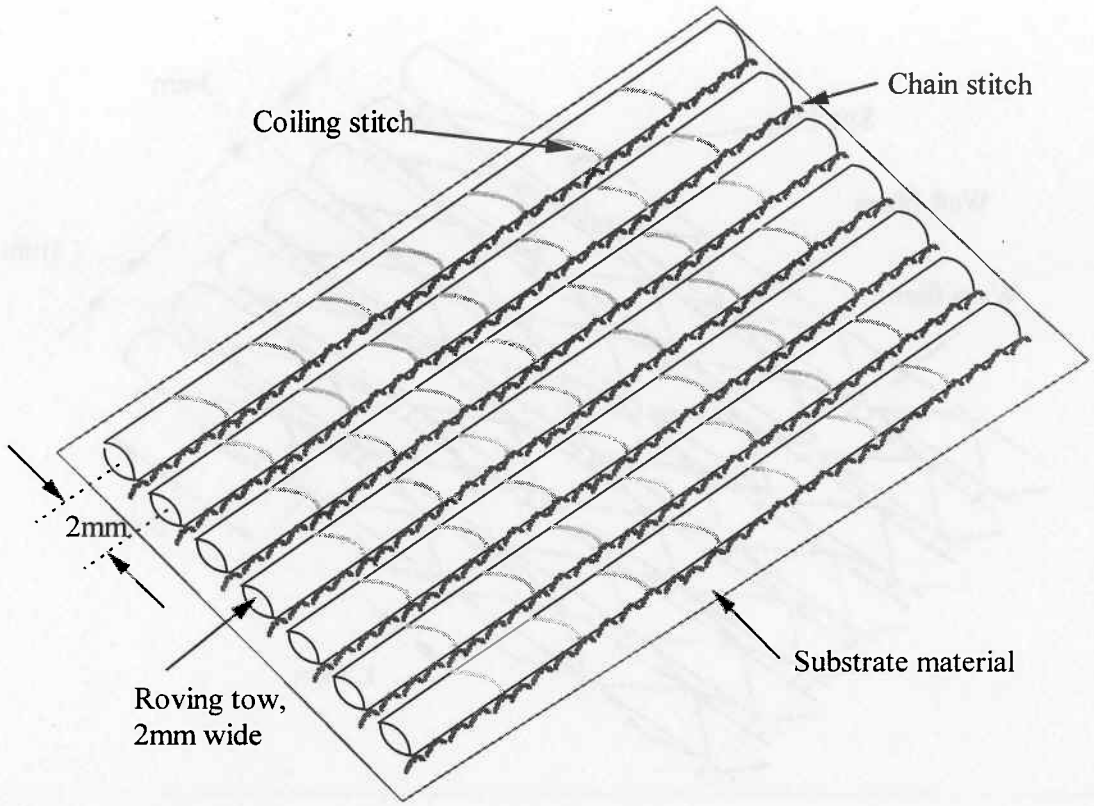

Figure 3: **Schematic structure of type B embroidered reinforcement, the helical wrapping stitch repeats every three chain-stitches.**

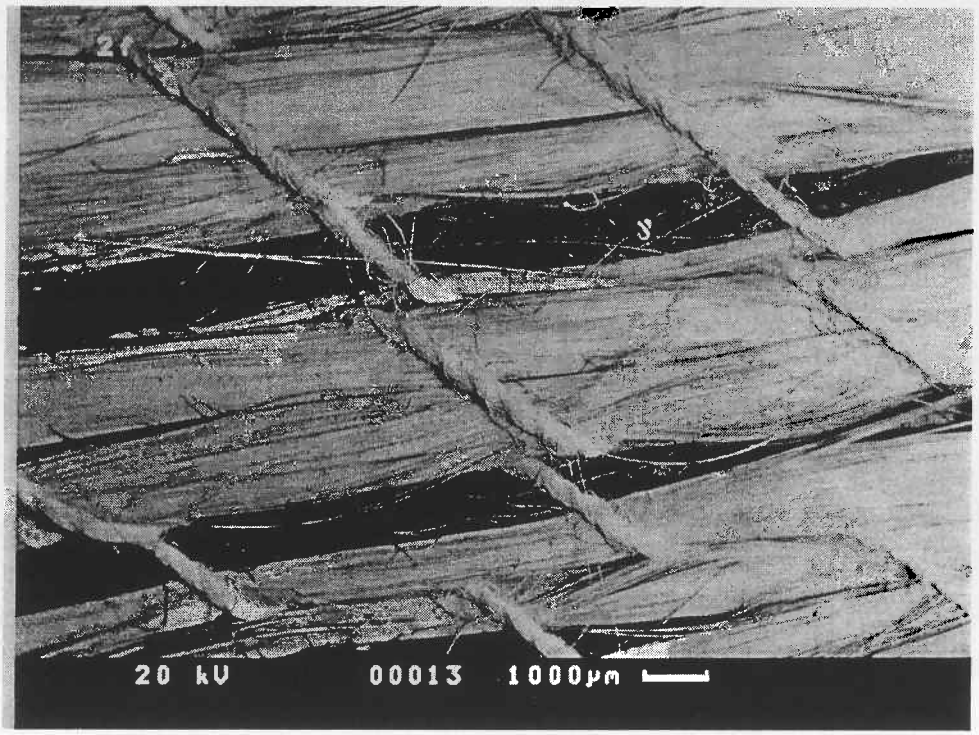

Figure 4: **Electron micrograph of type B embroidered reinforcement**

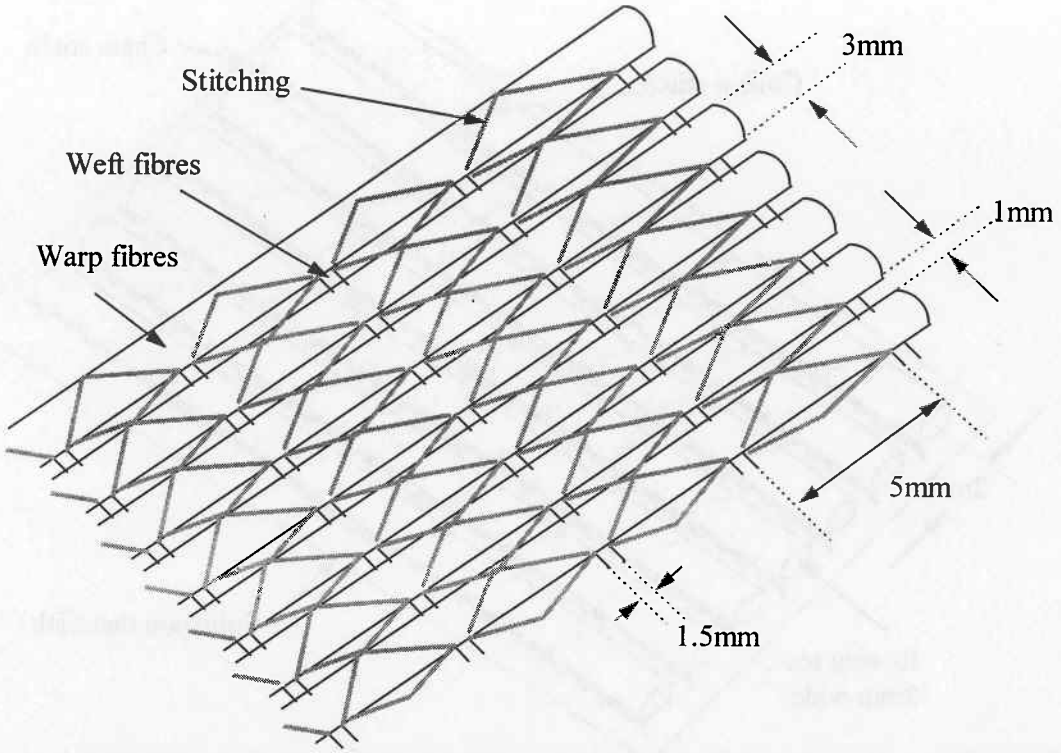

Figure 5: **Schematic structure of Tech Textiles E-LPb 567 quasi-unidirectional reinforcement.**

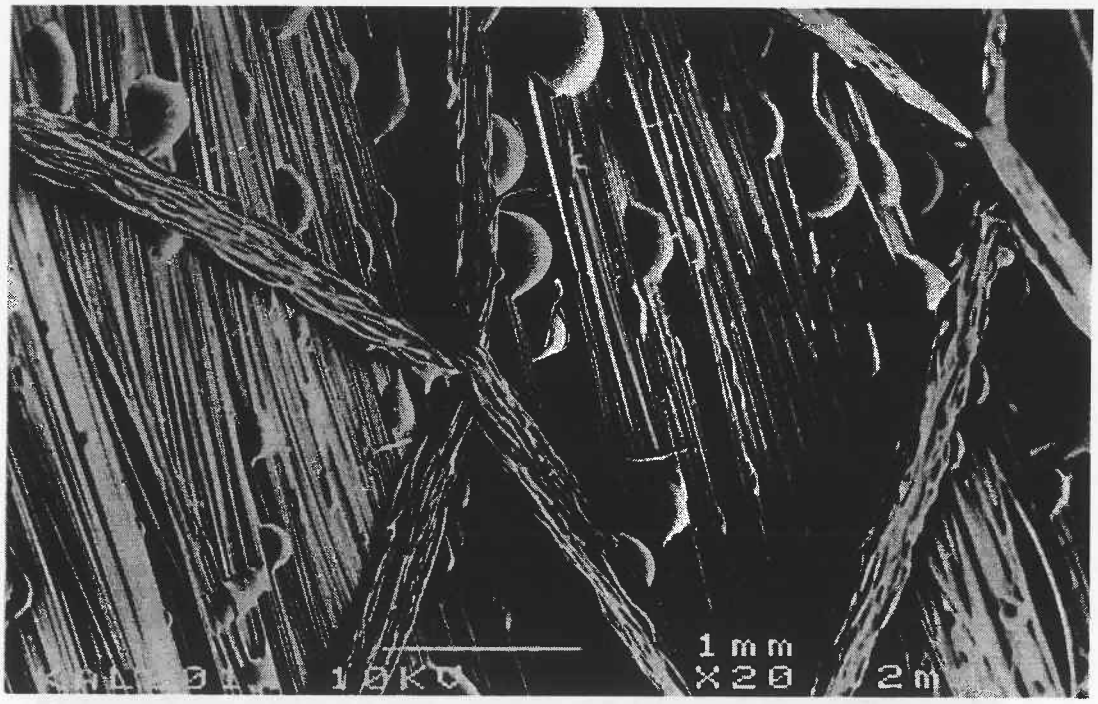

Figure 6: **Electron micrograph of Tech Textiles E-LPb 567 quasi-unidirectional reinforcement.**

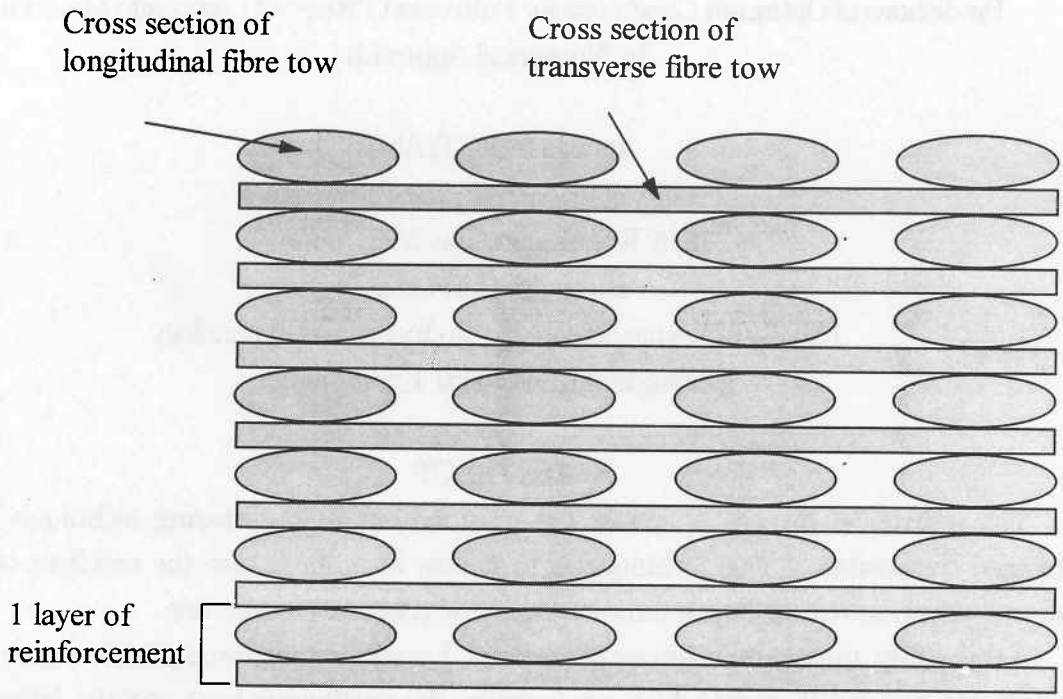

Figure 7: **Schematic cross-section of NCF preform showing stacking sequence and lay-up orientation.**

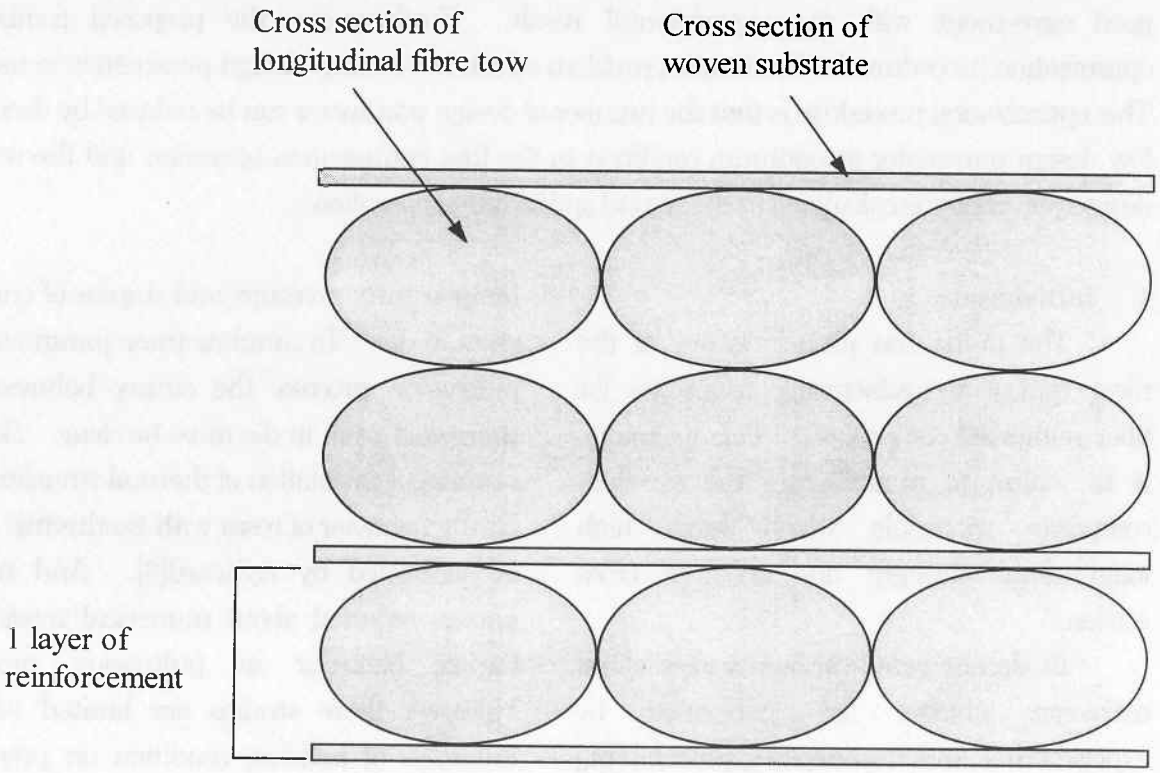

Figure 8: **Schematic cross-section of embroidered preform showing stacking sequence and lay-up orientation.**

Predictions of Optimum Conditions for Pultrusion Process of Composite Materials by Numerical Approach

Atsushi YOKOYAMA
Faculty of Education, Mie University
1515, Kamihama, Tsu, Mie, Japan
Hiroyuki, HAMADA
Faculty of Textile Science, Kyoto Institute of Technology
Matsugasaki, Sakyo-ku, Kyoto, Japan

ABSTRACT

The pultrusion process is one of the most typical manufacturing technique for fiber reinforced composites. This technique is to realize to manufacture the excellent composite materials which have high longitudinal strength and constant cross section.

In this study, the curing behavior of material during the pultrusion process was calculated by proposed numerical model which can consider the exothermic heat and the kinematics of resin. And the optimization procedure which can estimate simultaneously various optimum conditions of pultrusion process was proposed and evaluated by various conditions.

As a result, so that the validity of the proposed numerical model is confirmed in simulating the curing behavior of material in die during pultrusion process and the numerical result are good agreement with the experimental result. Furthermore, the proposed combined optimization procedure for the complex problem which have many design parameters is useful. This optimization procedure is that the number of design parameter can be reduced by deciding few design parameter as optimum condition in the first optimization operation and the rest of design parameter is calculated in the second optimization operation.

1. Introduction

The pultrusion process is one of the most typical manufacturing technique for fiber reinforced composites. This technique is to realize to manufacture the excellent composite materials which have high longitudinal strength and constant cross section.

In decent yeas, various studies about extrusion process are performed by experimental and numerical approach.[1][2] These studies mainly focused on behavior of materials in die and reported the viscosity, temperature, pressure and degree of cure of resin in die. To simulate these parameter in pultrusion process, the curing behavior of thermoset resin in die must be clear. So the numerical calculation of thermal transfer and curing behavior of resin with exothermic heat is performed by Aylward[3]. And many papers reported about numerical model for curing behavior in pultrusion process. However these studies are limited within influence of molding condition on pressure and pultrusion force in extrusion process, and there is few study which treat the optimum